Proceedings of the 2005 IEEE
International Conference on Robotics and Automation
Barcelona, Spain, April 2005

Realization by Biped Leg-wheeled Robot of Biped Walking and Wheel-driven Locomotion

Kenji Hashimoto, Takuya Hosobata, Yusuke Sugahara, Yutaka Mikuriya, Hiroyuki Sunazuka and Masamiki Kawase
Graduate School of Science and Engineering
Waseda University
Tokyo, Japan
hashimoto@suou.waseda.jp

Hun-ok Lim
Department of Mechanical Engineering
Kanagawa University
Kanagawa, Japan
Humanoid Robotics Institute, Waseda University

Atsuo Takanishi
School of Science and Engineering
Waseda University
Tokyo, Japan
Humanoid Robotics Institute, Waseda University

Abstract **- Biped walking is easily adaptable to rough terrain such as stairs and stony paths, but the walk speed and energy efficiency on the flat ground is not so effective compared with wheeled locomotion. In this paper, we propose a biped robot to be able to walk or wheel according to the ground conditions. For wheeled locomotion, WS-2 (Waseda Shoes - No.2) is developed which is composed of a DC motor, a spherical caster and two rubber pads on each foot. WS-2 is attached to the feet of WL-16 (Waseda Leg - No.16) that is the world's first biped-walking robot capable of carrying a human. Also, a path planning for wheeled locomotion is presented. Through hardware experiments, the effectiveness of this foot module is confirmed.**

Index Terms *- Wheel-driven Biped Robot; Biped Walking; Wheeled locomotion; Compensatory motion*

I. INTRODUCION

The advantages of biped locomotion in contrast to wheel-driven locomotion are particularly obvious in rough terrain. However, a disadvantage is that the legs of a biped robot support discontinuously its body and a support polygon generated by the feet is small in a swing phase. Also, its speed and energy efficiency on flat ground is not so effective. For stable locomotion, many researches on wheeled systems have been studied. The mechanism of wheeled robots adapting to rough terrain was proposed [1-3]. The passive suspension system was studied to deal with high terrain [4, 5].

Mobile robotic systems can be classified into two locomotion types. One is traditional mobile systems that move using only four wheels [6-9]. The other is a new locomotive system which can switch legged walk and wheeled movement according to the terrain. A biped robot mounted wheels was researched [10]. However, it is difficult to deal with stair because of stability problem. Also, the walking of the biped robot mounted on wheels has not yet studied.

Our objective is to develop a biped robot to be able to step over an obstacle and be able to move by wheels on the flat ground. If a biped robot has foot-wheeled system, its energy efficiency will be able to be improved and it will be able to move rapidly on flat plane using the wheel system. To realize biped locomotion and wheeled-locomotion according to terrain, walk-switching system is required. In this research, the hardware and the path generation of a wheeled foot system, WS-2 (Waseda Shoes - No.2), are described. Through hardware experiments, the effectiveness of the mechanism is confirmed.

This research was done in collaboration with TMSUK Co., Ltd. And also this research was supported by Fukuoka Prefecture, Fukuoka City, Kitakyushu City, SANYO Electric Soft Energy Co., Ltd., SolidWorks Japan K.K. and COSMOS Japan Co. Authors would like to express sincere thanks to them for their financial and technical supports.

II. HARDWARE OF WASEDA SHOES - NO. 2

WS-2 is a foot system that can convert biped walking into wheel-driven locomotion (see Figure 1). It consists of a spherical caster, a wheel and rubber pads. The rubber pads are attached to the inside of the foot, the active wheel that is driven by a DC motor is mounted on the front of the outer side of the foot, and the spherical caster is mounted on at the back of the outer side of the foot not to be constrained in a plain. If the foot is tilted to the outside, only the active wheel and the caster touch the ground. It makes a robot able to change biped walking to wheel-driven movement.

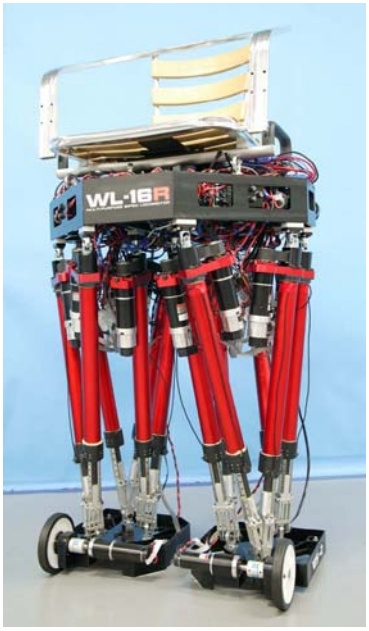

Figure 1. WS-2 / WL-16

WS-2 is designed as shown in Figure 2, using a finite element method system COSMOS. The specifications of WS-2 are shown in Table I. Its weight is 2.5 kg including DC motor (0.7 kg).

III. Wheel Driving Path Generation

We have studied about mechanism and control of biped walking robots since 1966 [11-13]. In this study, our complete walking pattern generation is used for a biped walking robot mounted on WS-2. For the biped robot to move using two wheels, a wheel driving path generation is added to the complete walking pattern generation as shown in Figure 3. Firstly, wheel motion is set using a Bezier curve, and the position of the foot is calculated. Secondly, a desired ZMP is planned near the center of a support polygon formed by four contact points of the sole. Thirdly, to cancel moments generated by the motion of the legs our previous moment compensation control method [14] is employed. Finally, complete walking pattern is determined including biped and wheel motion. How to generate a wheel trajectory is described below in detail.

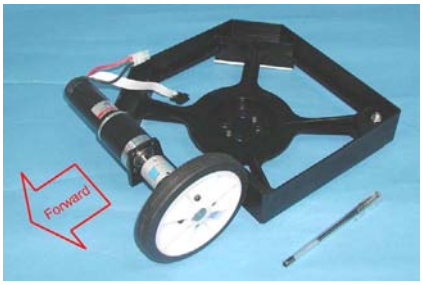

(a) Photograph

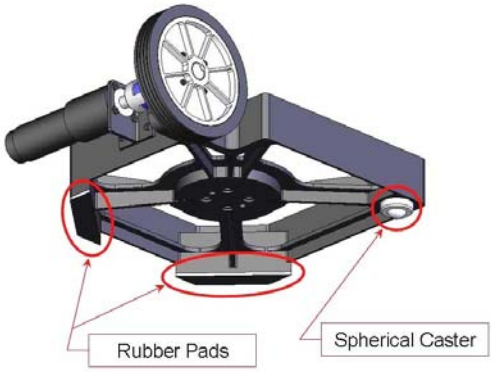

(b) Assembly drawing

Figure 2. Wheel-driven foot WS-2

TABLE I
WS-2 Specifications

Size	259×349×60 mm
Weight	2.5 kg
Wheel Diameter	130 mm
DC motor	90W (Nominal Voltage 42V)
Gear Reduction Ratio	26 : 1
Maximum Velocity	6.0 km/h

A. Constraints

It is not necessary to consider such a complicated condition as wheel slipping because the position and the direction of a robot in a plane are decided by angles of two wheels of WS-2. If a robot moves with rapid acceleration, there will be slipping motion between the wheels and the ground. However, we assume that there is no slipping in this research.

A world coordinate frame O is fixed on the ground where a biped walking robot mounted on WS-2 can move as shown in Figure 4. The position and the orientation of the robot can be described as follows:

$$\begin{aligned} \dot{x}_P &= \frac{1}{2} r\left(\dot{\theta}_R + \dot{\theta}_L\right)\cos\theta_P \\ \dot{y}_P &= \frac{1}{2} r\left(\dot{\theta}_R + \dot{\theta}_L\right)\sin\theta_P \\ \dot{\theta}_P &= \frac{1}{2}\frac{r\left(\dot{\theta}_R - \dot{\theta}_L\right)}{l} \end{aligned} \tag{1}$$

where $\left(x_P, y_p\right)$ is a position of a base point P of the robot with respect to O, θ_P is a direction of the robot, θ_R and θ_L are rotation angles of the right and left wheel, and r is the radius of wheel.

It is difficult to get arbitrary paths on a plane, because

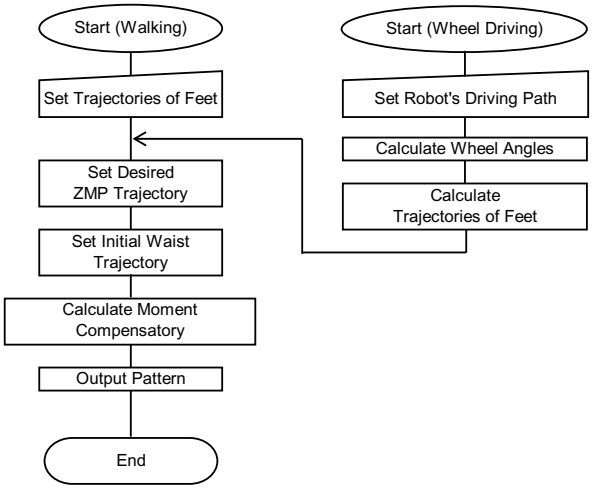

Figure 3. Flowchart of pattern generation

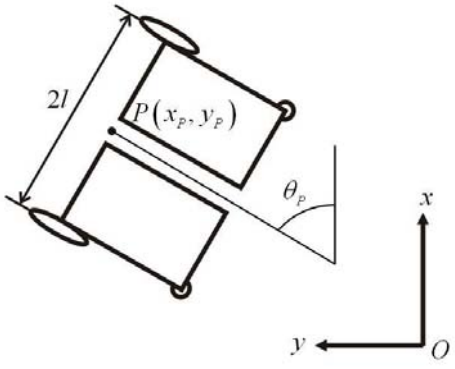

Figure 4. World coordinate frame

equation (1) has two inputs (θ_R , θ_L) and three outputs (x_P , y_P , θ_P). Eliminating $\dot{\theta}_R$ and $\dot{\theta}_L$ from equation (1), the following equation is obtained.

$$\frac{dy_P}{dx_P} = \tan\theta_P \tag{2}$$

To satisfy the non-holonomic constrains, the robot must always face to the tangential direction of the path.

B. Bezier Curve

In this study, a fifth order Bezier curve is used to set a robot's path as follows:

$$\mathbf{P}(s) = \sum_{i=0}^{n} \mathbf{P}_i B_i(s), \text{ when n=5} \tag{3}$$

where n is the order of Bezier curve, s is a parameter $(0 \le s \le 1)$, $\mathbf{P}_i$ is a control point (x_i , y_i), and $B_i(s) \equiv {}_nC_i \times s^i \times (1-s)^{n-i}$ is Bernstein function.

The initial and the final position of the Bezier curve are:

$$\mathbf{P}(0) = \mathbf{P}_0, \quad \mathbf{P}(1) = \mathbf{P}_5 \tag{4}$$

The slopes of the initial and the final position can be written as follows:

$$\frac{d\mathbf{P}}{ds}(0) = 5(\mathbf{P}_1 - \mathbf{P}_0), \quad \frac{d\mathbf{P}}{ds}(1) = 5(\mathbf{P}_5 - \mathbf{P}_4) \tag{5}$$

Noting equation (5), the slopes are individually decided by the second and the fifth control point. To connect some Bezier curves, the rate of change of the slopes (i.e. the rate of change of the robot's direction) should be continuous. Therefore, it is set to zero at the both ends of the curve.

$$\begin{aligned} &\frac{d^2\mathbf{P}}{ds^2}(0) = 0 \text{ , } \frac{d^2\mathbf{P}}{ds^2}(1) = 0 \\ &\Rightarrow \mathbf{P}_2 = 2\mathbf{P}_1 - \mathbf{P}_0 \text{ , } \mathbf{P}_3 = 2\mathbf{P}_4 - \mathbf{P}_5 \end{aligned} \tag{6}$$

As noted above, four control points are needed to define a fifth order Bezier curve. As a matter of convenience, parameters are defined as shown in TABLE II. A robot's path determined by the above method is given in Figure 5.

C. Path Mapping

A path connected by Bezier curves is a two-dimensional curve related to a mediation variable. So, the velocity of the robot at every position of the path should be given. If the mediation variables are projected onto the time, the path can be expressed as follows:

$$\begin{aligned} &\left(x_P(s), y_P(s)\right) = \mathbf{P}(s) \\ &\theta_P(s) = \angle\dot{\mathbf{P}}(s) \\ &s = f(t) \end{aligned} \tag{7}$$

The mapping function $f(t)$ is determined using a fifth order polynomial with six constraints such as position, velocity and acceleration. Employing this method, velocity and acceleration at random passing points can be specified. We assume that acceleration at any connection points is zero, because it is difficult for a human to decide the acceleration intuitively. Only velocity at each passing points is specified.

$$\begin{aligned} &f(t) = f_n\left(t - \sum_{i=0}^{n-1} T_i\right) + \sum_{i=0}^{n-1} f_i(T_i) \\ &f_n(r) = \sum_{j=0}^{5} a_{nj} r^j \\ &\left(\sum_{i=0}^{n-1} T_i \le t < \sum_{i=0}^{n} T_i\right) \end{aligned} \tag{8}$$

where T_n is the time moving from the n-th pass point to the (n+1) pass point, and a_{nm} is the coefficient of the m-th term of the n-th function.

Coefficients of the equation (8) are given as follows:

$$\begin{aligned} a_{n0} &= s_n \\ a_{n1} &= \dot{s}_n \\ a_{n2} &= 0 \\ a_{n3} &= \frac{2}{T_n^3}\left\{5(s_{n+1} - s_n) - T_n(2\dot{s}_{n+1} + 3\dot{s}_n)\right\} \\ a_{n4} &= \frac{1}{T_n^4}\left\{-15(s_{n+1} - s_n) + T_n(7\dot{s}_{n+1} + 8\dot{s}_n)\right\} \\ a_{n5} &= \frac{3}{T_n}\left\{2(s_{n+1} - s_n) - T_n(\dot{s}_{n+1} + \dot{s}_n)\right\} \end{aligned} \tag{9}$$

where s_n is a parameter corresponding to the n-th passing point.

In this method, we pay attention to zero velocity at a connection point of a forward and a backward path.

D. Calculation of Wheel Angles

For a robot to move along the robot's path generated above, the angles of the right and left wheel must be calculated. The contact points of the right and left wheel are fixed with respect to the base point P as shown in Figure 4.

TABLE II
DEFINITION OF PARAMETERS

	Forward Driving Path		Backward Driving Path	
	s=0	s=1	s=0	s=1
Position	$(x_0, y_0) \equiv \mathbf{P}_0$	$(x_T, y_T) \equiv \mathbf{P}_5$	$(x_0, y_0) \equiv \mathbf{P}_0$	$(x_T, y_T) \equiv \mathbf{P}_5$
Direction	$\theta_0 \equiv \angle(\mathbf{P}_1 - \mathbf{P}_0)$	$\theta_T \equiv \angle(\mathbf{P}_5 - \mathbf{P}_4)$	$\theta_0 \equiv \angle(\mathbf{P}_0 - \mathbf{P}_1)$	$\theta_T \equiv \angle(\mathbf{P}_4 - \mathbf{P}_5)$
Constant	$c_0 \equiv \lvert\mathbf{P}_1 - \mathbf{P}_0\rvert$	$c_T \equiv \lvert\mathbf{P}_5 - \mathbf{P}_4\rvert$	$c_0 \equiv \lvert\mathbf{P}_0 - \mathbf{P}_1\rvert$	$c_T \equiv \lvert\mathbf{P}_4 - \mathbf{P}_5\rvert$

So, if a position and a direction of the robot are known, the contact positions of the wheels can be set (see Figure 5).

By integrating the length of each trajectory, wheel angle is calculated (see Figure 6). However, because the length of each trajectory does not include wheel angle data, the rotation direction of the wheels must be included in the integration.

$$\phi_R(t) = \frac{1}{r}\int \sigma_R(t)\, dL_R$$
$$dL_R = \sqrt{dx_R^{\,2} + dy_R^{\,2}} = \sqrt{\left(\frac{dx_R}{dt}\right)^2 + \left(\frac{dy_R}{dt}\right)^2}\, dt \qquad (10)$$

where $\phi_R(t)$ is a rotation angle of wheel, (x_R, y_R) is the position of $\mathbf{P}_R(t)$, and $\sigma_R(t) \equiv sign\left(\dot{\mathbf{P}}_R(t)\right)$ is the function determining the rotation direction of wheel.

E. Switching between Biped Walking and Wheel Driving

In wheel driving mode, only wheels and casters touch the ground because the feet are tilted to the outside. Therefore, the robot can move on the ground freely (see Figure 7). To tilt both feet, each foot should be rotated around the edge formed by the wheel and the spherical caster.

Consider only the right leg in switching locomotion modes. Suppose that four points of the foot contact the ground. Frame $\{A\}$ is fixed on a contact point of the wheel, and frame $\{P\}$ is fixed on a base point of the robot as shown in Figure 8 (a). The homogeneous transform, ${}^{P}_{A}\mathbf{T}$, which describes the frame $\{A\}$ relative to the frame $\{P\}$ is written as follows:

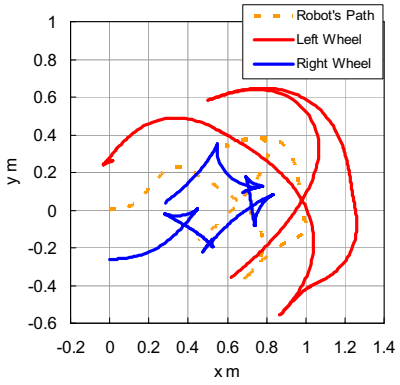

Figure 5. A robot's path generated by five Bezier curves and wheel traiectories

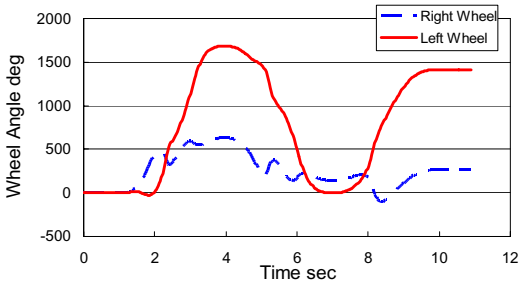

Figure 6. Wheel angles

$${}^{P}_{A}\mathbf{T} = \begin{bmatrix} 1 & 0 & 0 & 0 \\ 0 & 1 & 0 & -l \\ 0 & 0 & 1 & 0 \\ 0 & 0 & 0 & 1 \end{bmatrix} \qquad (11)$$

The origin of frame $\{B\}$ is fixed on the contact point of the foot which is coincident with the origin of frame $\{A\}$ as shown in Figure 8 (b). The transform of $\{B\}$ relative to $\{A\}$ is as follows:

$${}^{A}_{B}\mathbf{T} = \begin{bmatrix} 1 & 0 & 0 & 0 \\ 0 & \cos\theta_{tilt} & -\sin\theta_{tilt} & 0 \\ 0 & \sin\theta_{tilt} & \cos\theta_{tilt} & 0 \\ 0 & 0 & 0 & 1 \end{bmatrix} \qquad (12)$$

where θ_{tilt} is an inclination angle of foot.

Frame $\{C\}$ is fixed on the center of the foot as shown in Figure 8 (a). The position and the posture of the foot are represented on frame $\{C\}$. In this research, the origin of frame $\{C\}$ is coincident with the point projected the origin of coordinate system of a force/torque sensor onto the

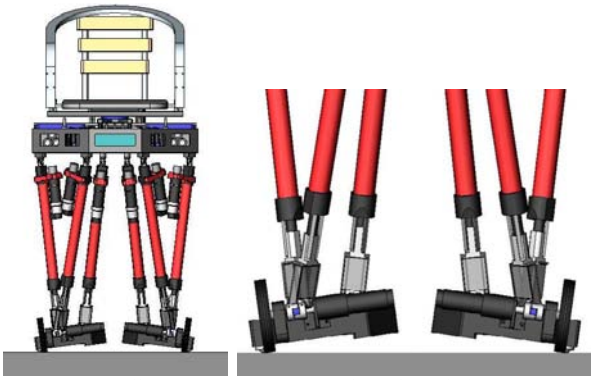

(a) Overall view (b) Enlarged view

Figure 7. Basic position in wheel driving mode

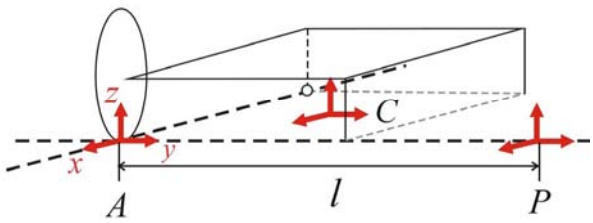

(a) Frame $\{A\}$, $\{C\}$ and $\{P\}$

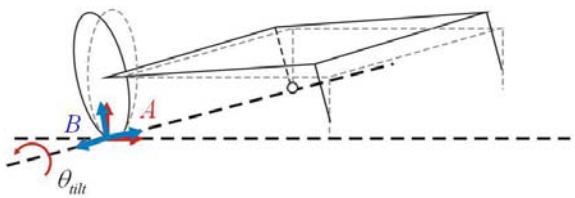

(b) Frame $\{B\}$

Figure 8. Four coordinate frames

support polygon formed by the foot.

The relative position between the wheel and the foot doesn't change before and after tilting the foot. Therefore, frame $\{D\}$ representing the position and the orientation of the tilted foot is described as follows:

$$ {}^{B}_{D}\mathbf{T} = {}^{A}_{C}\mathbf{T} \tag{13} $$

Also, the transform of the tilted foot relative to $\{P\}$ can be written as follows:

$$ {}^{P}_{D}\mathbf{T} = {}^{P}_{A}\mathbf{T}\,{}^{A}_{B}\mathbf{T}\,{}^{B}_{D}\mathbf{T} = {}^{P}_{A}\mathbf{T}\,{}^{A}_{B}\mathbf{T}\,{}^{A}_{C}\mathbf{T} \tag{14} $$

F. Setting Trajectory of Foot

The position and the orientation of the foot with respect to a world coordinate frame $\{O\}$ are described as follows:

$$ {}^{O}_{P}\mathbf{T} = \begin{bmatrix} {}^{O}_{P}\mathbf{R} & {}^{O}\mathbf{P}_{PORG} \\ 0\ \ 0\ \ 0 & 1 \end{bmatrix} $$
$$ {}^{O}_{P}\mathbf{R} = \begin{bmatrix} \cos\theta_P & -\sin\theta_P & 0 \\ \sin\theta_P & \cos\theta_P & 0 \\ 0 & 0 & 1 \end{bmatrix} \tag{15} $$
$$ {}^{O}\mathbf{P}_{PORG} = \begin{bmatrix} x_P \\ y_P \\ 0 \end{bmatrix} $$

From equation (14) and (15), the trajectory of the foot is obtained as follows:

$$ {}^{O}_{D}\mathbf{T} = {}^{O}_{P}\mathbf{T}\,{}^{P}_{D}\mathbf{T} \tag{16} $$

IV. Experimental Tests and Consideration

The robot foot proposed in this research is universally designed. It is able to be applicable to all biped robots. To evaluate the foot system, four experiments are conducted using the multi-purpose biped locomotor WL-16 (Waseda Leg - No.16) [14, 15]. Firstly, the robot moves 1 m forward from a standstill state and stops. In this experiment, the locomotion velocity is 0.3 m/s when the robot moves without slipping. Also, maximum velocity is about 0.61 m/s and maximum acceleration is about 1.7 m/s^2. As shown in Figure 9, measured ZMPs are deviated from reference ZMPs especially near to acceleration and deceleration points because of moment errors caused by mechanical deflection. Considering that X length of a support polygon is about ± 150 mm, we can see that the ZMP errors are not so much large. However, if the robot is accelerated more, its wheels will begin slipping.

Secondly, experiment of switching locomotion is conducted using a rectangle plate of 900 mm W × 73 mm H as follows:

(i) the robot moves to the front of the rectangle plate using its wheels,
(ii) steps on the plate using its biped legs, moves to the edge of the plate using its wheels,
(iii) steps down the plate using its biped legs and moves to the original position using its wheels.

Switching locomotion between biped walking and wheel driving is achieved by using WS-2. The sequential photographs of this experiment are shown in Figure 10.

Thirdly, the energy consumption of wheel driving is compared with that of biped walking. Wheel locomotion has the same movement distance (0.7 m) and time (7.68 s) as biped walking. The robot in the biped walking mode walks 8 steps with a step length of 0.10 m and a walking cycle of 0.96 s/step.

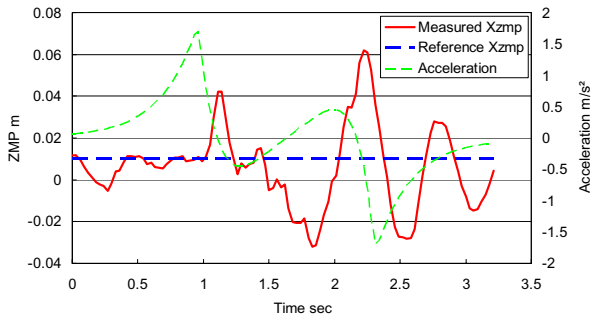

Figure 9. ZMP trajectory

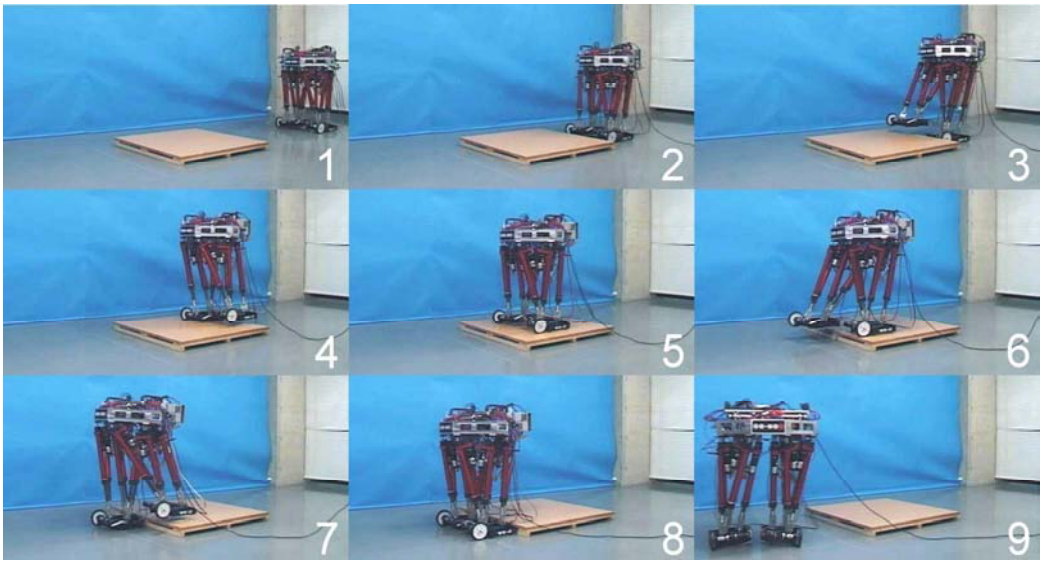

Figure 10. Switching between biped walking and wheel driving

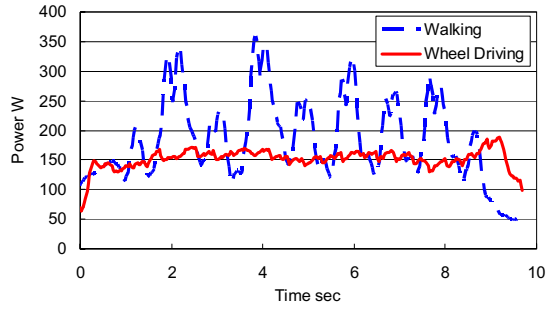

Figure 11. Comparison of energy consumption

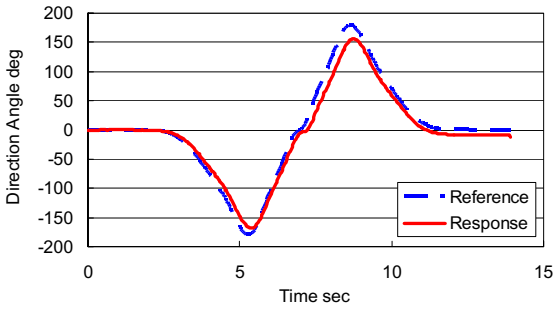

Figure 12. Waist direction angle

The energy consumption in case of biped walking is 1740 J, while the energy consumption is 1470 J in case of wheel driving as shown in Figure 11. We can see that energy saving of about 15 % is achieved. Energy consumption even in the wheel driving mode is not so small because the joint motors of the legs should support the robot body. If the negative operation electromagnetic brakes of WL-16 [15] are used during locomotion, energy consumption can be reduced.

Finally, we determine an 8-type driving path (see Section III). The robot moves on the path. In this experiment, the mechanism is verified using directional angles measured by the waist posture sensor because the robot has not a system measuring its position with respect to absolute coordinate frame. Figure 12 shows a waist direction angle history when moving the path. We can see that the robot moves along the reference path with a maximum error of 30 degrees. The deviation is due to a slip between the wheels and the ground.

V. Conclusions and Future Work

We have developed a biped robot with wheeled feet, WS-2, to deal with biped walk and wheeled locomotion. WS-2 consists of a spherical caster, a wheel and rubber pads. Through various experiments using WL-16 mounted on WS-2 are conducted on a flat plane. Locomotion switching between a biped walk system and a wheel system according to terrain is realized. Also, high speed movement and whirling motion is achieved using WS-2. Experimental results show that energy consumption of a biped robot is reduced by switching between biped walk and wheeled locomotion depending on terrain. Through hardware experiments, the effectiveness of this foot module is confirmed.

It is difficult for the robot to deal with disturbances because a real-time balance control is not considered. This is our future work.

Acknowledgment

This study has been conducted as part of the humanoid project at the Humanoid Robotics Institute, Waseda University. The authors would like to thank Mr. Akihiro Ohta and Mr. Chiaki Tanaka for their help in conducting experiments.

References

[1] E. Rollins, J. Luntz, A. Foessel, B. Shamah, and W. Whittaker, "Nomad: a demonstration of the transforming chassis," Proc. of the IEEE ICRA 1998, pp. 611-617, Leuven, Belgium, May, 1998.

[2] R. Volpe, "Rocky 7: A next generation mars rover prototype," *Journal of Advanced Robotics*, vol. 11, no. 4, pp. 341-358, 1997.

[3] S. Hirose, E. Fukushima, R. Damoto, and H. Nakamoto, "Design of terrain adaptive versatile crawler vehicle HELIOS-VI," Proc. of the IEEE/RSJ IROS, pp. 1540-1545, Maui, Hawaii, USA, November, 2001.

[4] L. Matthies, Y. Xiong, R. Hogg, D. Zhu, A. Rankin, B. Kennedy, M. Herbert, R. Maclachlan, C. Won, T. Frost, G, Sukhatme, M. McHenry, and S. Goldberg, "A Portable, Autonomous, Urban Reconnaissance Robot," Proc. Sixth Int. Conf. on Intelligent Autonomous Systems, 2000.

[5] T. Estier, Y. Crausaz, B. Merminod, M. Lauria, R. Piguet, and R. Siegwart, "An innovative space rover with extended climbing abilities," in *International Conference on Robotics in Challenging Environments*, Albuquerque, USA, 2000.

[6] G. Endo and S. Hirose, "Study on Roller-Walker (Multi-mode Steering Control and Self-contained Locomotion)," Proc. of the IEEE ICRA 2000, pp. 2808-2814, San Francisco, USA, 2000.

[7] A. Halme, I. Leppanen, S. Salmi, and S. Ylonen, "Hybrid locomotion of a wheel-legged machine," in *International Conference on Climbing and Walking Robots*, Madrid, Spain, 2000.

[8] F. Michaud, et. al, "AZIMUT, a Leg-Track-Wheel Robot," Proc. of the IEEE/RSJ IROS 2003, pp. 2553-2558, Las Vegas, USA, October, 2003.

[9] C. Grand, F. BenAmar, F. Plumet and P. Bidaud, "Decoupled control of posture and trajectory of the hybrid wheel-legged robot Hylos," Proc. of the IEEE ICRA 2004, pp. 5111-5116, New Orleans, USA, April, 2004.

[10] O. Matsumoto, S. Kajita and K. Komoriya, "Flexible Locomotion Control of a Self-contained Biped Leg-wheeled System," Proc. of the IEEE/RSJ IROS 2002, pp. 2599-2604, Lausanne, Switzerland, October, 2002.

[11] J. Yamaguchi, A. Takanishi and I. Kato, "Development of a Biped Walking Robot Adapting to a Horizontally Uneven Surface," Proc. of the IEEE/RSJ IROS 1994, pp. 1156-1163, Munich, Germany, September, 1994.

[12] A.Takanishi, M.Ishida, Y.Yamazaki, and I.Kato, "The realization of dynamic walking by the biped walking robot," Proc. of the IEEE ICRA 1985, pp.459-466, St.Louis, USA, March, 1985.

[13] A.Takanishi, T.Takeya, H.Karaki, M.Kumeta, and I.Kato, "A control method for dynamic walking under unknown external force," Proc. of the IEEE/RSJ Int. Workshop on Intelligent Robots and Systems, pp.795-801, Tsuchiura, Japan, July, 1990.

[14] Y. Sugahara, T. Endo, H. O. Lim and A. Takanishi, "Control and experiments of a multi-purpose bipedal locomotor with parallel mechanism," Proc. of the IEEE ICRA 2003, pp. 4342-4347, Taipei, Taiwan, September, 2003.

[15] Y. Sugahara, T. Hosobata, Y. Mikuriya, H. Sunazuka, H.O. Lim and A. Takanishi, "Realization of Dynamic Human-Carrying Walking by a Biped Locomotor," Proc. of the IEEE ICRA 2004, pp. 3055-3060, New Orleans, USA, April, 2004.